ELECTRIC CURRENT MODULATION BY GATE FREQUENCY IN A QUANTUM RING NANOTRANSISTOR

Martin Konôpka, Peter Bokes

Department of Physics, Institute of Nuclear and Physical Engineering, FEI STU, Slovak University of Technology in Bratislava, Ilkovičova 3, 812 19 Bratislava
E-mail: martin.konopka@stuba.sk

Received 24 May 2013; accepted 27 May 2013

1. Introduction

Nano-sized electronic devices are subject of intense research because of their attractive properties for applications in electronics and spintronics. One of the key capabilities of many electronic devices is to quickly switch electric current between two significantly different levels. Atomic-scale devices are promising candidates for this purpose. Their fast operation is facilitated by their small dimensions and their energy efficiency. In addition, specific quantum effects can be utilised, namely the quantum interference effect. In 2006, the concept of the Quantum-Interference Effect Transistor (QuIET) has been proposed [1, 2], a ring-shaped device promising extremely fast operation. In our recent works we developed a new theoretical and computational method for description of time-dependent electronic transport through nanoscale devices [3, 4, 5]. The method is based on the stroboscopic wave packets and presently is implemented within a tight-binding (TB) model and uses the independent-electron approximation. The electrons in our approach precisely satisfy the Pauli exclusion principle however. Among other target systems, we have applied the formalism to description of the dynamical operation of the QuIET [6], i.e. its response to abrupt gate-potential turn-on and off. In Ref. [5] we considered the effect of the harmonic gate on such quantum ring. We have found that for certain setups the *average* electric current depends on the gate frequency. The dependence on the frequency is oscillatory itself.

The model of the gate application used in Refs. [6, 5] was a very simple one: the on-site energies of affected ring atoms were modified, i.e. the prescription $\Delta\epsilon_l(t) = eV_{\rm g}(t)$ has been used and the quantum dynamics of the system was solved with these modified atomic energies. In this equation l is the site (atom) index, $\Delta\epsilon_l$ is the gate-induced equilibrium variation of the atomic on-site energy, $V_{\rm g}(t)$ is the gate potential which can be an arbitrary function of time and e is the unit charge. The gate potential was applied to a chosen part (one branch) of the ring atoms.

In general, a gate represents an additional lead for the system which apart from shifting the on-site energies does also exchange electrons with the system. In this work we will present results for such a dynamical gate – lead and discuss its implications on the effect found before using only the time-dependent on-site energies [5, 6]. In addition, our present results are obtained using a generalised stroboscopic wave-packet method which uses stroboscopic wave packets for wavefunctions in the leads and localised atomic orbitals for wavefunctions in the device [7].

2. Description of the studied model

One of the simplest realisations of the QuIET is an atomic ring which we model as a ring of electronic sites with TB couplings (see Fig. 1). (The size of the system shown on

the figure is only illustrative; see the caption.) All atoms in the system are of the same kind, characterised by the equilibrium on-site energy ϵ. Only nearest neighbours are directly coupled, as described by the TB hopping parameter $t_{\rm B}$ [5, 6], same for almost all nearest neighbours. In our convention $t_{\rm B}$ takes a negative value and we use the quantity $|t_{\rm B}|$ as the unit of energy. The interaction between the gate electrode and the ring is allowed to take a generally different value $t_{\rm GR}$ however. The simulation protocol used to obtain our results is as follows: (i) First 500 units

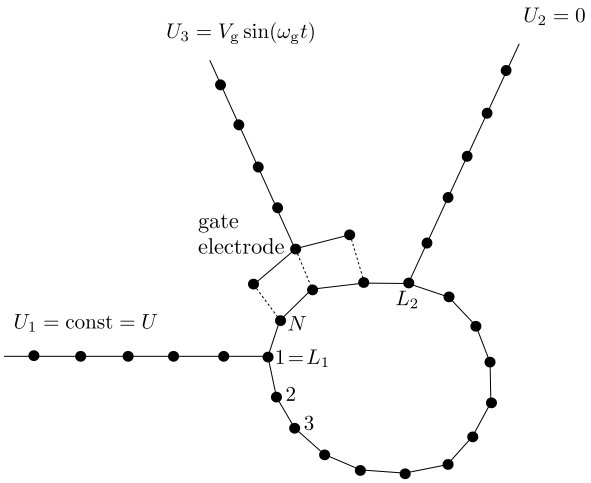

Fig. 1: *Schematic view on the model under study. The sketched numbers of atoms in the figure are only illustrative. The ring size N used in our calculations is 80. The atoms of the ring are indexed by labels 1, 2, ..., N, as shown in the scheme. Special indices are L_1, L_2 and L_3. They indicate which ring atoms are attached to the leads. In case of the gate electrode all of the atoms $L_2 + 1, \ldots, N$ are attached to respective gate electrode atoms. In our simulations we use $L_2 = 71$ which means that 9 of the ring atoms are affected by the gate potential. The gate electrode itself also consists of 9 atoms.*

of time is used for equilibration, i.e. the system undergoes a time evolution without any bias or gate potential. (ii) After the equilibration period the statical bias $U_1 = 0.5\,|t_{\rm B}|/e$ is abruptly turned on at the time $t_{\rm sw} = 500\,\hbar/|t_{\rm B}|$. (iii) After next 300 time units (a period sufficient to reach a quasi-stationary regime) the sinusoidal bias is applied to lead 3 (see Fig. 1).

All atoms of the gate lead *and* of the gate electrode itself have their on-site energies lifted by the time-dependent amount

$$eU_3(t) = V_{\rm g}\sin(\omega_{\rm g}t) \tag{1}$$

relative to the equilibrium level ϵ. Lead 2 is kept at the constant zero bias as shown on Fig. 1. In our model the effect of the gate electrode on the ring is such that the affected ring atoms have their on-site energies lifted by

$$\Delta\epsilon_l^{\rm gate}(t) = \left(\frac{t_{\rm GR}}{t_{\rm B}}\right)^2 eU_3(t)\ . \tag{2}$$

(Only those ring atoms that are connected by the dashed lines in Fig. 1 are affected by the gate.) In addition, all the ring atoms have a contribution to their on-site energy due to the bias in the lead 1,

$$\Delta\epsilon_l^{\rm bias} = \frac{1}{2}\,eU\ , \tag{3}$$

i.e. the average between the biases in leads 1 and 2 [5].

3. Results

Using the gate potential one can control the electric current through the device. The most desirable type of control is switching the device between its on and off states [6, 5]. However, here we will demonstrate a different functionality: we will show that the amplitude of the averaged current is modulated by the frequency of the gate potential. In Fig. 2 we show detailed time-dependent currents as they will later help to interpret our results and also demonstrate capabilities of our approach to theoretical and computational quantum transport analysis. The

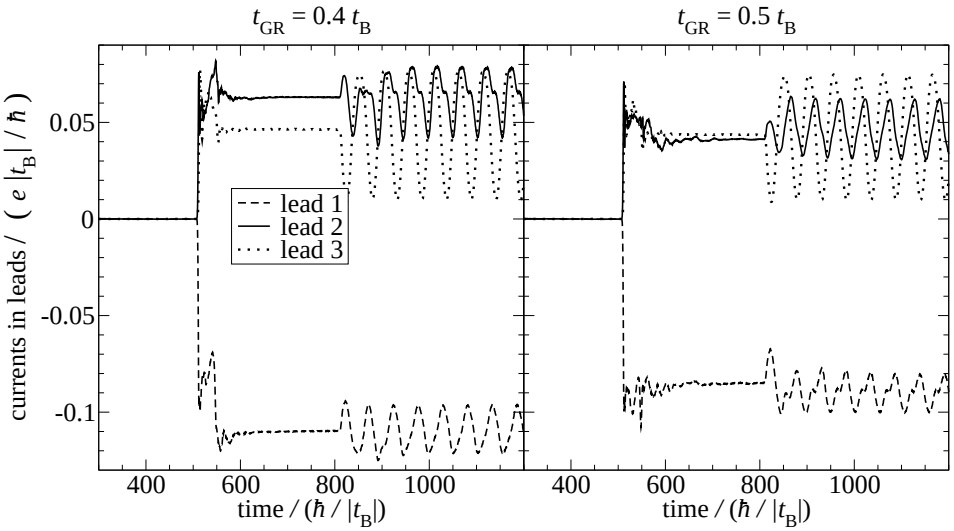

Fig. 2: *Typical time-dependent currents in the studied system, which is the ring of* $N = 80$ *atoms with lead attachment sites* $L_1 = 1$ *and* $L_2 = 71$ *(see caption to Fig. 1). The sign convention in this figure (not in next two ones) is such that a current flowing into the device (the ring) is negative. The currents have been computed at sites 20 lattice parameters away from the ring. For these particular examples we have used the the statical bias value of* $U = 0.5\,|t_{\rm B}|/e$*, gate amplitude* $V_{\rm g} = 0.15\,|t_{\rm B}|/e$ *and the gate angular frequency* $\omega_{\rm g} = 0.12\,|t_{\rm B}|/\hbar$*. The parameters used for the two graphs differ by the gate-ring coupling matrix element* $t_{\rm GR}$ *values of which are shown in multiplies of* $t_{\rm B}$*.*

effect of the sinusoidal gate applied to electrode 3 is reflected by an oscillating electron current through the leads. Responses on the applied harmonic gate are generally anharmonic, although for other values of $\omega_{\rm g}$ they can be close to harmonic functions. Because the gate electrode has a fully conductive lead attached to it, there is a significant current flowing through it. For currents varying slowly in time the three currents sum up to zero. For significantly time-dependent currents only their time-averaged values fulfil this property.

In Fig. 3 we show main results from our model. Plots within particular graph use the same value of bias U and the gate amplitude $V_{\rm g}$. Legends indicate different magnitudes of the gate-ring coupling parameter $t_{\rm GR}$. For convenience in this type of figures we plot the current values through lead 1 using the positive sign, i.e. opposite to Fig. 2. We see the noticeable modulation of the time-averaged current through lead 1 for certain values of the gate-ring coupling $t_{\rm GR}$, e.g. for $t_{\rm GR} = 1.0\,t_{\rm B}$ and $t_{\rm GR} = 0.5\,t_{\rm B}$. Decreased coupling leads to suppression of the modulation. The exception is the coupling value $t_{\rm GR} = 0.5\,t_{\rm B}$, for which the time-averaged current also exhibits significant modulation, at least for lower gate frequencies. We see from

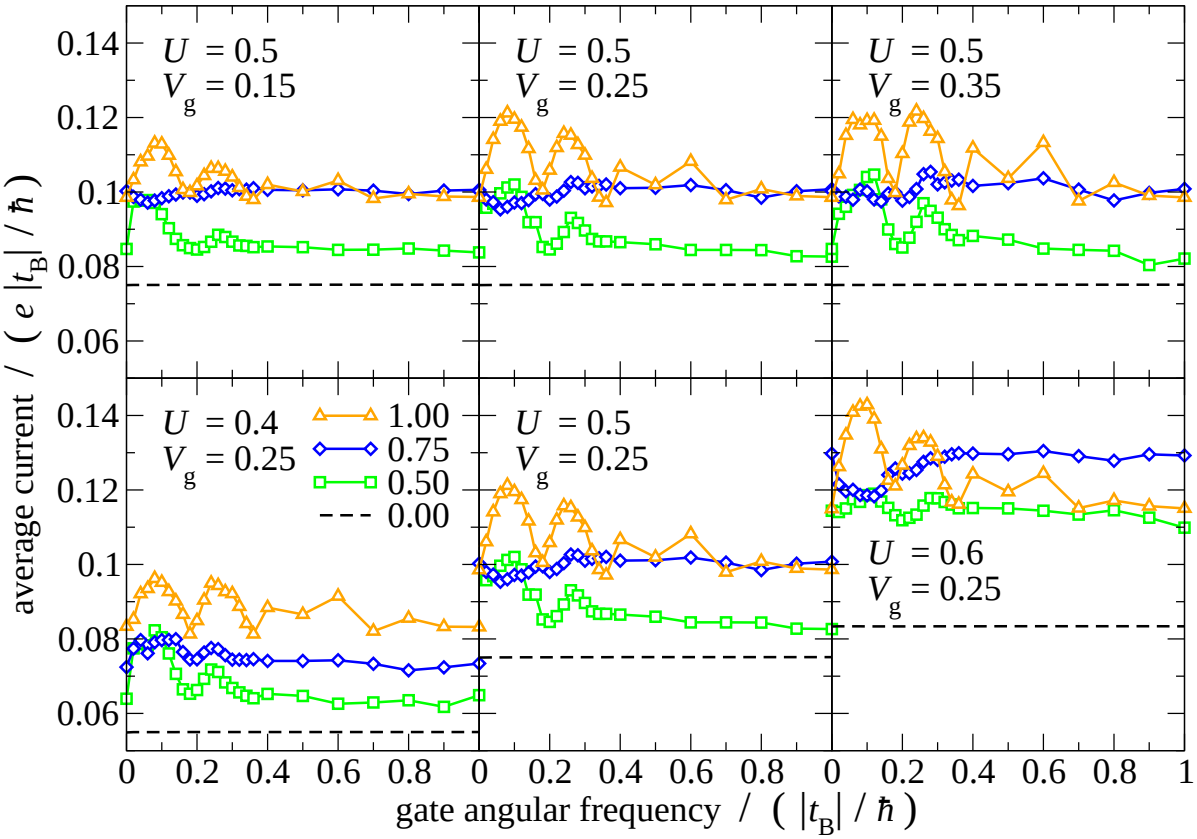

Fig. 3: *Time-averaged currents through lead 1, now conveniently taken as positive quantities. Graphs in the upper row use the same value of bias ($U = 0.5\,|t_\mathrm{B}|/e$) and different values of the gate amplitude V_g. Graphs in the lower row use the same gate amplitude ($V_\mathrm{g} = 0.25\,|t_\mathrm{B}|/e$) while the bias value U varies between individual graphs. The plot with $U = 0.5\,|t_\mathrm{B}|/e$ and $V_\mathrm{g} = 0.25\,|t_\mathrm{B}|/e$) is displayed twice for convenience. The key to line types indicates particular relative values $t_\mathrm{GR}/t_\mathrm{B}$ of the gate-ring coupling parameter. Other parameters like the ring size are the same as used also for Fig. 2.*

the graphs that the positions of the peaks in the averaged currents are only marginally sensitive to the applied parameters U and V_g.

We finalise our results by showing the plot of the average current as dependent on the t_GR coupling at a fixed value of the gate frequency $\omega_\mathrm{g} = 0.5\,|t_\mathrm{B}|/\hbar$. The other parameters are $U = 0.5\,|t_\mathrm{B}|/e$ and $V_\mathrm{g} = 0.15\,|t_\mathrm{B}|/e$. Resulting dependence is plotted in Fig. 4. We can notice the wide dip around the coupling value $t_\mathrm{GR} = 0.5\,t_\mathrm{B}$, in agreement with previously shown results. (Here it is important to notice that the scale on the vertical axis starts at the value of 0.07.) Two detailed time-dependent currents which have been used to compute the averages (the points at $\omega = 0.4\,|t_\mathrm{B}|/\hbar$ and $0.5\,|t_\mathrm{B}|/\hbar$) are shown in Fig. 2. The non-trivial dependence on the coupling results from the interplay of several effects. One of them is the electron tunnelling through the barrier. The other is the quantum interference of electron amplitudes transmitted by different ring branches. The barrier height in the gated ring branch depends quadratically on the coupling. Higher barrier tends to lower conductance of a particular channel, here the ring branch. However, it also affects the phase of an electron wavefunction in the gated branch and consequently impacts the interference pattern which means either suppression or increase of currents in individual leads. In addition the internal energy levels of the ring are effectively broadened by the increased coupling which also impacts the overall transmittance. Hence the

current *vs.* coupling dependence plotted on Fig. 4 results from several effects which can either act constructively or compensate each other.

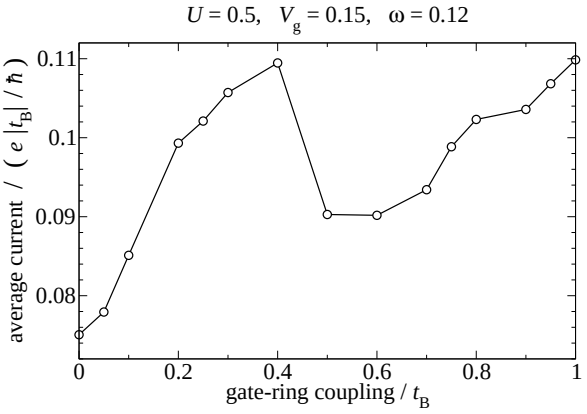

Fig. 4: *The time-averaged currents in lead 1 versus the magnitude of the gate-ring coupling* t_{GR}. *The other parameters are indicated on the top of the graph. The geometry of the ring is the same as used for Figs. 2 and 3.*

4. Conclusion

We presented a computational study of a dynamical gate effect applied to a tight-binding model of a ring-shaped quantum-interference nanotransistor. Compared to our former analysis, we used a model of the gate that not only controls on-site energies of the atoms but can also transfer electrons to or from the device. We have found that the electric current is modulated by the gate frequency also in this more general model. The simulations have been performed using our home-developed generalised stroboscopic wave packet approach which is very suitable for open systems and time-dependent effects.

Acknowledgements

This work was supported in parts by the Slovak Research and Development Agency under the contract No. APVV-0108-11 and by the Slovak Grant Agency for Science (VEGA) through grant No. 1/0372/13.

References:

[1] D. M. Cardamone, C. A. Stafford, S. Mazumdar, *Nano Lett.* **6**, 2422 (2006).

[2] C. A. Stafford, D. M. Cardamone, S. Mazumdar, *Nanotechnology* **18**, 424014 (2007).

[3] P. Bokes, F. Corsetti, R. W. Godby, *Phys. Rev. Lett.* **101**, 046402 (2008).

[4] P. Bokes, *Phys. Chem. Chem. Phys.* **11**, 4579 (2009).

[5] M. Konôpka, P. Bokes, *Eur. Phys. J.* B **86**, 114 (2013).

[6] M. Konôpka, P. Bokes, In: *Proceedings of the 18th International Conference on Applied Physics of Condensed Matter*, ISBN 978-80-227-3720-3 (Štrbské Pleso, 2012).

[7] M. Konôpka, P. Bokes, in preparation.